PAIN® 153 (2012) 1450–1458

PAIN®

www.elsevier.com/locate/pain

Hyperalgesia by low doses of the local anesthetic lidocaine involves cannabinoid signaling: An fMRI study in mice

Simone C. Bosshard [a,b], Joanes Grandjean [a,b], Aileen Schroeter [a], Christof Baltes [a], Hanns U. Zeilhofer [b,c,d], Markus Rudin [a,b,c,*]

[a] Institute for Biomedical Engineering, University and ETH Zurich, Zürich 8093, Switzerland
[b] Neuroscience Center, University and ETH Zurich, Switzerland, Zürich 8057, Switzerland
[c] Institute of Pharmacology and Toxicology, University of Zurich, Zürich 8057, Switzerland
[d] Institute of Pharmaceutical Sciences, ETH Zurich, Zürich 8093, Switzerland

Sponsorships or competing interests that may be relevant to content are disclosed at the end of this article.

ARTICLE INFO

Article history:
Received 21 June 2011
Received in revised form 29 March 2012
Accepted 2 April 2012

Keywords:
Functional magnetic resonance imaging
Mice
Lidocaine
Hyperalgesia
Cannabinoid receptor CB_1

ABSTRACT

Lidocaine is clinically widely used as a local anesthetic inhibiting propagation of action potentials in peripheral nerve fibers. Correspondingly, the functional magnetic resonance imaging (fMRI) response in mouse brain to peripheral noxious input is largely suppressed by local lidocaine administered at doses used in a clinical setting. We observed, however, that local administration of lidocaine at doses 100× lower than that used clinically led to a significantly increased sensitivity of mice to noxious forepaw stimulation as revealed by fMRI. This hyperalgesic response could be confirmed by behavioral readouts using the von Frey filament test. The increased sensitivity was found to involve a type 1 cannabinoid (CB_1) receptor-dependent pathway as global CB_1 knockout mice, as well as wild-type mice pretreated systemically with the CB_1 receptor blocker rimonabant, did not display any hyperalgesic effects after low-dose lidocaine. Additional experiments with nociceptor-specific CB_1 receptor knockout mice indicated an involvement of the CB_1 receptors located on the nociceptors. We conclude that low concentrations of lidocaine leads to a sensitization of the nociceptors through a CB_1 receptor-dependent process. This lidocaine-induced sensitization might contribute to postoperative hyperalgesia.

1. Introduction

Sensory and nociceptive processing involves a network of neural structures, the first element being the nociceptor, a high threshold sensory neuron connecting peripheral tissues with the central nervous system (CNS) [41]. In the brain, nociceptive processing activates the "pain matrix" involving structures such as somatosensory, insular, cingulate, and prefrontal cortices, thalamus, and periaqueductal gray [3]. Functional magnetic resonance imaging (fMRI), assessing changes in cerebral blood oxygenation levels (BOLD [blood oxygen level-dependent] [35]), has been used for studying pain processing both in humans and animals, mostly in rats [8,11,27,29,31,32] but recently also in mice [1,5,18]. Mice are attractive, as transgenic lines may yield information on mechanisms underlying pain signaling. Substantial progress has been made in understanding the molecular mechanisms of normal or pathological pain states, much of it with the help of genetically engineered mice displaying altered sensitivity to noxious input [9,16,24,34].

Although sodium channel block and action potential inhibition by high concentrations of lidocaine are well established, effects of low concentrations are considerably more complex [28] and their effects on central pain processing have not been characterized in detail. fMRI can help to further elucidate effects of lidocaine on modulating sensory processing in response to peripheral noxious stimuli [28,42]. It has been reported that lidocaine applied intravenously at low doses in rats enhances fMRI responses to acute nociceptive stimulation [28]. Several pharmacological effects could account for this increased sensitivity. In addition to inducing local anesthesia through blockade of voltage-gated sodium channels, lidocaine has been reported to inhibit tandem pore domain potassium channels [23]. Leffler et al. [25] showed that lidocaine directly activates and sensitizes the transient receptor potential channel 1 (TRPV1) located on C fibers and activated by noxious chemical or physical stimuli [10].

We have applied fMRI in mice using an electrical forepaw stimulation paradigm [5] to study effects of lidocaine treatment

* Corresponding author. Address: Institute for Biomedical Engineering, Animal Imaging Center, Wolfgang-Pauli-Str. 27, Zurich 8093, Switzerland. Tel.: +41 44 633 76 04; fax: +41 44 633 11 87.
E-mail address: rudin@biomed.ee.ethz.ch (M. Rudin).

0304-3959/$36.00
http://dx.doi.org/10.1016/j.pain.2012.04.001

on the BOLD response. Local administration of lidocaine at clinical doses (2%) largely inhibited activation of the CNS pain matrix. Yet, pretreatment with lidocaine using doses 100-times lower prompted a hyperalgesic effect as reflected both by increased BOLD-fMRI responses to electrical forepaw stimulation and by behavioral readouts. Based on recent studies [14,37], we hypothesized that activation of type 1 cannabinoid (CB_1) receptors might contribute to this hyperalgesia. Activation of CB_1 receptors was reported to facilitate the action of TRPV1 receptors, thereby increasing the excitability of nociceptors [14]. Furthermore, activation of CB_1 receptors in the dorsal horn during strong nociceptive input was shown to cause disinhibition of pain-specific dorsal horn neurons, rendering them excitable by input from nonnociceptive A fibers, which might result in hyperalgesia in areas surrounding the original nociceptive input [37]. We have therefore investigated the effect of modulating CB_1 signaling on lidocaine-induced hyperalgesia using genetically engineered mice lacking the CB_1 receptor globally ($CB_1^{-/-}$ mice) [30] and by pharmacological inhibition in wild-type (WT) mice using the specific CB_1 receptor blocker rimonabant. To further pin down the location of relevant CB_1 receptors, nociceptor-specific CB_1 receptor knockout mice (*sns*-$CB_1^{-/-}$) [2] have been included in the study.

2. Material and methods

2.1. Animals and stimulation paradigm

All experiments were performed in accordance with the Swiss law of animal protection. Sixty female C57BL/6 mice (including littermates of transgenic animals), 8 female global $CB_1^{-/-}$ mice (provided by B. Lutz and G. Marsicano, Max-Planck-Institute of Psychiatry, Munich, Germany), and 10 (5 males and 5 females) nociceptor-specific *sns*-$CB_1^{-/-}$ mice (provided by R. Kuner, University of Heidelberg, Germany) were used for the experiments. The mice were anesthetized with isoflurane (Abbott, Cham, Switzerland; induction at 2%–3%, maintenance at 1.2% in a 70% air – 30% oxygen mixture), endotracheally intubated, mechanically ventilated using a breathing rate of 90 breaths per minute, and paralyzed (for more details refer to [5]). The tail vein was cannulated for drug administration, and body temperature was maintained at 36.5° ± 0.5°C using a warm-water circuit integrated into the animal support (Bruker BioSpin AG, Fällanden, Switzerland). Heart rate and blood oxygenation were monitored using an MR-compatible infrared sensor (MouseOx Pulse Oximeter; Starr Life Sciences, Oakmont, PA, USA). For electrical stimulation, a pair of needle electrodes (Genuine Grass Instruments, West Warwick, RI, USA) was inserted subcutaneously into the distal and proximal end of the palm of each forepaw, with a distance of 2–3 mm between the 2 needles. Electrical stimulation was carried out using the following parameters (for details see [5]): current amplitude 1.5 mA, frequency 3 Hz, pulse duration 0.5 ms, with 4 stimulation periods of 60 seconds duration (corresponding to 180 pulses) followed by resting periods of 120 seconds duration. The initial baseline period lasted 120 seconds (Fig. 1b). Stimulation amplitudes of <1 mA were considered nonnoxious [5].

2.2. Experimental groups

The study design consisted of 4 sets of experiments: 1) Effects of lidocaine in WT mice: 10 μL of lidocaine hydrochloride dissolved in 0.9% NaCl was injected into the left forepaw 40 minutes prior to electrical stimulation. The following lidocaine doses were administered: 1.5 nmole, 3.0 nmole, 4.5 nmole, 6.0 nmole, or 700 nmole (corresponding to 0.42, 0.81, 1.23, 1.62, and 190 μg lidocaine hydrochloride, respectively). The pH of the injected solution was 6.3–6.4 for an amount of lidocaine $\leqslant$ 6 nmole and 5.1 for an amount of 700 nmole lidocaine per 10 μL. As control groups, naïve animals that were not injected with any substance and mice injected into the right forepaw with 10 μL of saline solution (0.9% NaCl, pH 6.4) have been used. In order to exclude potential noxious stimulation due to stimulation of pH-sensitive receptors, additional experiments have been carried out in mice receiving local injections of 10 μL phosphate-buffered saline (PBS, pH 7.4) and 3 nmole lidocaine dissolved in 10 μL PBS (pH 7.3). 2) Effects of lidocaine in $CB_1^{-/-}$ mice: at first, experiments with electrical stimulation only were carried out to test for intrinsic differences between naïve $CB_1^{-/-}$ and WT animals. In a second experiment, 3 nmole lidocaine in a volume of 10 μL and 10 μL of 0.9% NaCl were injected into the left forepaw and right forepaw, respectively, prior to electrical stimulation. 3) Pharmacological inhibition of CB_1 using rimonabant: the CB_1 antagonist/inverse agonist rimonabant (SR 141716, Anawa Trading SA, Wangen, Switzerland) [26] was dissolved in a mixture of ethanol, Cremaphor (Sigma-Aldrich, Steinheim, Germany), and 0.9% NaCl (1:1:18) and administered intravenously (10 mg/kg) 20 minutes prior to electrical stimulation. fMRI experiments were carried out in animals that had received no further treatment or in mice that had been pretreated with 3 nmole of lidocaine. The control group received an intravenous administration of vehicle in addition to the local pretreatment with 3 nmole of lidocaine. 4) Effects of lidocaine in *sns*-$CB_1^{-/-}$ mice: 3 nmole lidocaine in 10 μL, and 10 μL of 0.9% NaCl were injected into the left forepaw and right forepaw, respectively, 40 minutes prior to electrical stimulation. fMRI experiments were also performed without pretreatment in *sns*-$CB_1^{-/-}$ to test for intrinsic differences in the fMRI response as compared to WT animals.

The numbers of animals for the various experimental groups are given in Table 1. The high numbers of animals in the group receiving 3 nmole lidocaine (n = 28) and in the naïve control group with electrical stimulation only (n = 21) are due to control experiments, which were conducted with each set of experiments to avoid working with historical controls only. In addition, WT littermates of all transgenic animals were also measured and pooled with the data collected on WT mice.

2.3. MRI equipment and sequences

All MRI experiments were performed on a Bruker BioSpec 94/30 small-animal MR system (Bruker BioSpin MRI, Ettlingen, Germany) operating at 400 MHz (9.4 Tesla). For signal transmission and detection, a commercially available cryogenic quadrature RF surface probe (CryoProbe), consisting of a cylinder segment (180° coverage, radius 10 mm) and operating at a temperature of 30 K was used (Bruker BioSpin AG, Fällanden, Switzerland; for detailed information see [4]). Anatomical reference images in coronal and sagittal directions (slice orientations are given using the nomenclature of the mouse brain atlas [15]) were acquired using a spin echo (Turbo-RARE) sequence with the following parameters: field-of-view = 20 × 20 mm^2, matrix dimension = 200 × 200, slice thickness = 0.5 mm, interslice distance = 0.7 mm, repetition delay = 3500 ms, echo delay = 13 ms, effective echo time = 39 ms, rapid acquisition with relaxation enhancement (RARE) factor (number of echoes sampled for each excitation) = 32, and number of averages = 1. The coronal slices for the fMRI experiment were positioned and oriented on the basis of these anatomical reference images using both sagittal and horizontal images to adjust the proper slice position and angulation with regard to the magnet coordinate system in order to best fit the mouse atlas sections [15] with the center of the 0.5-mm-thick MRI section to correspond to location of the atlas section. BOLD-fMRI data were acquired using a gradient-echo echo planar imaging (EPI) sequence with the following parameters: five coronal slices covering a range of 2–5 mm anterior

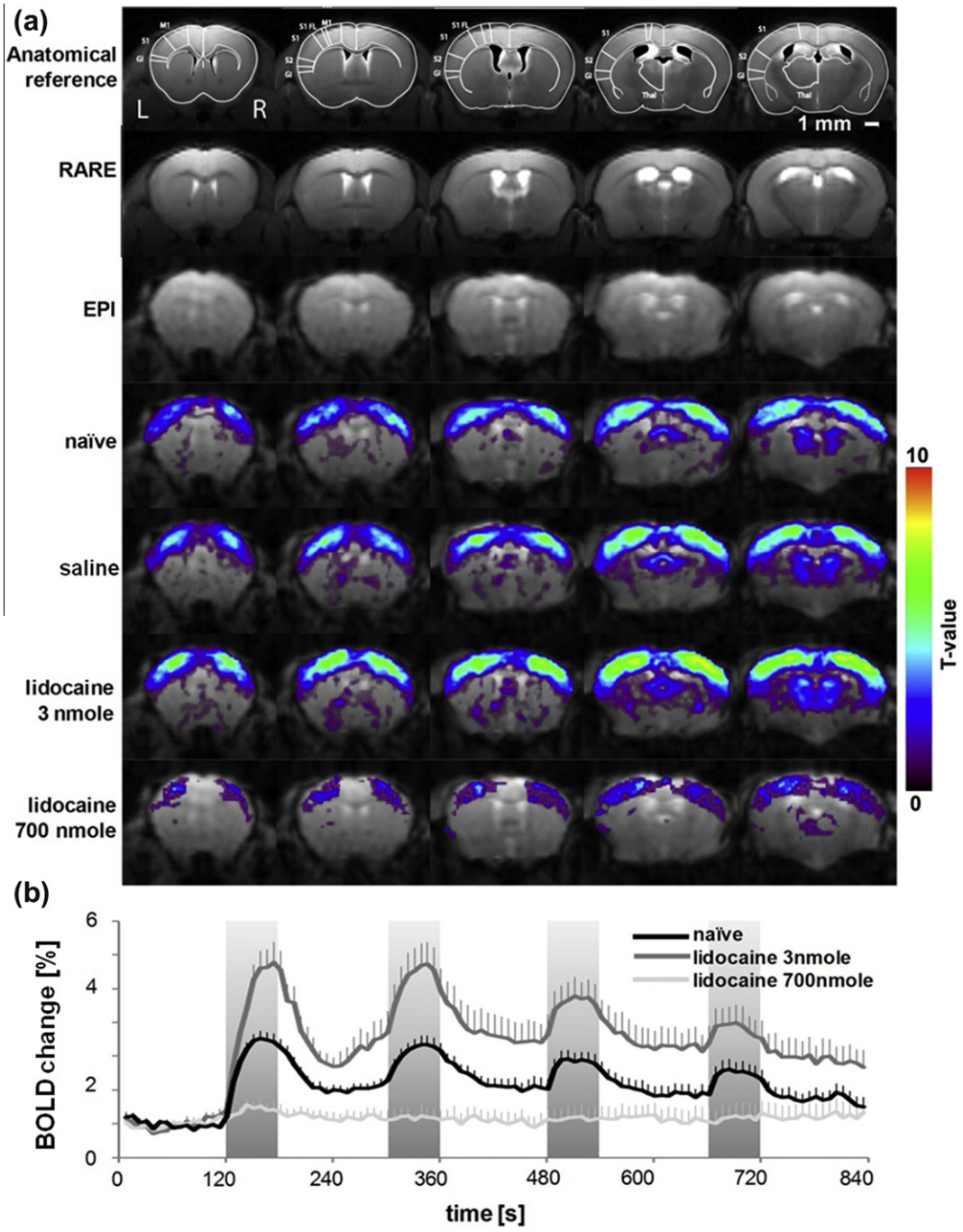

Fig. 1. Activation maps and temporal blood oxygen level-dependent (BOLD) signal profile. (a) The top 3 lines display the anatomical reference images from the mouse brain atlas, the structural magnetic resonance images obtained using the rapid acquisition with relaxation enhancement (RARE) sequence and the echo planar imaging (EPI) images for the 5 coronal slices recorded (central slice position at 5.1, 4.4, 3.7, 3.0, and 2.3 mm rostral to the interaural line, left to right). Regions labeled on the anatomical reference image: S1, S1 front limb (S1 FL), S2, granular insular cortex (GI), and thalamus (Thal). Both the RARE and the EPI data set have been spatially normalized to the brain atlas (see Section 2). Activation maps derived from general linear model (GLM) analysis are shown as overlay on EPI images for naïve animals ("naïve"), mice pretreated by injection of 10 μL of saline into the forepaw ("saline"), 3 nmole ("lidocaine 3 nmole"), and 700 nmole of lidocaine dissolved in 10 mL ("lidocaine 700 nmole:). Color-coded overlays show the mean activated regions across all animals obtained from GLM analysis (family-wise error corrected, threshold at $P < 0.05$, minimum cluster size of 10 voxels). The color bar shows the respective T-value ranging from 0 to 10; L and R indicate left and right on the image; the scale bar represents a distance of 1 mm. (b) Temporal profile of the relative change of the BOLD signal intensity as observed in the contralateral S1 area during electrical forepaw stimulation. Traces show response to electrical stimulation in naïve animals (black), after local injection of 3 nmole (dark gray) and after injection of 700 nmole of lidocaine (light gray). Gray bars indicate stimulation periods. All values are indicated as mean ± SEM.

to the interaural line (IAL +2–5 mm) were recorded with field-of-view = 23.7 × 12.0 mm^2, matrix dimension = 90 × 60 (acquisition) and 128 × 64 (reconstruction), yielding an in-plane resolution of 200 × 200 μm^2, slice thickness = 0.5 mm, interslice distance = 0.7 mm, repetition delay = 2500 ms, echo delay = 8.5 ms, and number of averages = 3 (averaging in k-space) resulting in an image acquisition time of 7.5 seconds. The fMRI experiment comprised either 112 repetitions lasting 840 seconds (Fig. 1b) or 152 repetitions lasting 1140 seconds (prolonging the recovery period following the last stimulation period).

Table 1
Overview of experimental groups used.

Strain	Systemic application	Local administration at forepaw (volume 10 μL)				
		Naïve	Saline	PBS	Lidocaine (in saline)	
					Dose [nmole/mouse]	
WT		21	6*	5	*1.5*	8
					3	28
					3+	5
					4.5	7
					6	7
					700	6
	Rimonabant	4			*3*	5
	Vehicle rimonabant				*3*	5
$CB_1^{-/-}$		6	8*		*3*	8
sns-$CB_1^{-/-}$		6	10*		*3*	10

Numbers indicate size of respective groups. Saline, phosphate-buffered saline (PBS), or lidocaine was injected into the forepaw of the mouse using an injection volume of 10 μL. The lidocaine dose is given in italics. The type 1 cannabinoid (CB_1) antagonist rimonabant or the respective vehicle was administered intravenously.

* (Saline groups) indicates that functional magnetic resonance imaging experiments following saline and lidocaine pretreatment were carried out using the same animals.

+ The group receiving lidocaine dissolved in PBS.

2.4. Data analysis and statistics

EPI images are susceptible to distortions due to differences in local susceptibility values. These distortions were accounted for in part by applying a bilinear scaling procedure. Each coronal EPI cross-section was scaled along 2 orthogonal directions to best fit the coordinate system of the mouse brain atlas [15]. The origin of the coordinate system was defined by the midline point at the base of the brain. A right-handed coordinate system was then defined for each coronal EPI image by choosing the ventral-to-dorsal direction of the brain midline as *y*-axis and the direction perpendicular to the midline pointing into the right hemisphere as *x*-axis. The lengths of the vectors from the base to the dorsal edge of the brain ($y_{EPI;i}$) and from the midline to the edge of the right hemisphere at its widest point ($x_{EPI;i}$) was compared with the respective dimensions obtained from the mouse brain atlas ($x_{atlas,i}$ $y_{atlas,i}$), yielding the linear scaling factors $c_{xi} = x_{atlas,i}/x_{EPI;i}$ and $c_{yi} = y_{atlas,i}/y_{EPI;i}$. These scaling factors were then used to match EPI images to the respective cross-sections from the mouse atlas using IDL-based software developed in-house [38].

Following co-registration, nonbrain structures were manually removed using Biomap software (M. Rausch, Novartis, Basel, Switzerland). Images were smoothed using a 280-μm^3 Gaussian smoothing kernel using SPM 5 (FIL Methods Group, London, UK) and SPMmouse plug-in (Wolfson Brain Imaging Centre, Cambridge, UK). Following this procedure, a general linear model (GLM) analysis was performed using SPM 5. The model was derived from the first activation peak using a block design convoluted with a finite impulse function and high-pass filtered with a cutoff of 500 seconds. GLM assesses correlations on a pixel-by-pixel basis between the fMRI signal and the stimulation pattern. Activation was detected using a family-wise error-corrected statistical threshold of $P = 0.05$ for all experiments and a minimal cluster size of 10 voxels. For quantitative analyses of BOLD signal changes, regions-of-interest were selected based on their location in the mouse brain atlas [15]. BOLD signal changes are displayed in percent of the baseline value prior to the stimulation. GLM-derived activation patterns were used for group analysis.

Comparative statistics was performed taking the maximal amplitude of the BOLD signal change of the first stimulation period (from 120 to 180 seconds, see Figs. 1, 3 and 4b) of each animal. Values were tested at the $\alpha = 0.05$ level using the nonparametric Kruskal-Wallis test followed by the post hoc Fisher test (comparison between different groups). All values are presented as mean (across animals) ± SEM.

2.5. Behavioral test: von Frey filaments

The behavioral testing was performed in 19 WT mice, which were kept in the test cages for 1 hour prior to testing to allow accommodation. For baseline recording, each mouse was tested on each forepaw for 15 minutes, obtaining at least 3 data points per paw and per 5-minute interval, measuring paw withdrawal thresholds to stimulation with electronically controlled von Frey filaments. Following the baseline, either 3 nmole lidocaine (n = 11) dissolved in 10 μL or the same amount of saline (n = 8) was injected into both forepaws. This was done under short isoflurane anesthesia (2%, 1–2 minutes), after which the animals were put back into the test boxes. Measurements were taken during 55 minutes after lidocaine or saline injection in all animals. Values were averaged for intervals of 5 minutes and are presented as mean (across animals) ± SEM. Statistical analysis was performed using the nonparametric Kruskal-Wallis test followed by the post hoc Bonferroni test ($\alpha = 0.05$ level, comparison between different groups).

3. Results

3.1. Pretreatment with low doses of lidocaine causes hyperalgesia

Electrical stimulation of the forepaw using a current amplitude of 1.5 mA was shown to activate brain areas attributed to the pain matrix [11]. Consistent BOLD responses have been observed in the areas of the primary and secondary somatosensory cortices (S1 and S2), the motor cortex, the thalamus, and the insular cortex as revealed by GLM analysis and displayed in the activation maps obtained for the 5 sections recorded (Fig. 1a). The BOLD signal response to unilateral forepaw stimulation appeared consistently bilateral in all activated regions as it has been described previously [5]. The temporal changes of the BOLD amplitude in the regions involved corresponded well with the 4 stimulation periods (Fig. 1b for S1 area contralateral to the stimulated paw, black line for naïve mice). The BOLD signal intensity increased significantly at each stimulus onset, but there was a net decrease of the BOLD signal amplitude for subsequent stimulation periods across the 4-block cycle. Also, the signal did not return to the initial baseline level within the 2-minute resting interval following a stimulation episode, but remained elevated until the start of the next stimulation block, in line with earlier observations [5]. Noninvasive physiological monitoring of the mice showed stable parameters throughout the entire experiment: no changes in body temperature (36.5 ± 0.5°C) and arterial O_2 saturation (>98%) could be detected during

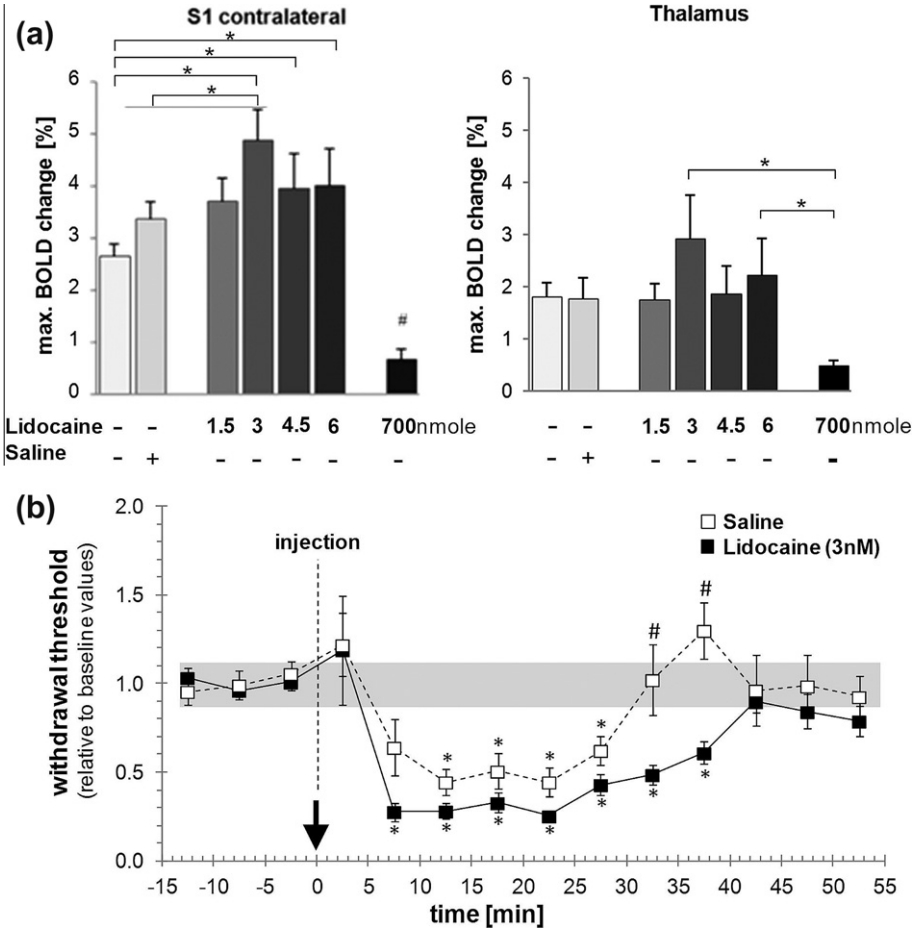

Fig. 2. Pretreatment with low concentrations of lidocaine leads to an increase in blood oxygen level-dependent (BOLD) signal. (a) Maximum amplitude of BOLD signal changes in the S1 contralateral to the stimulated paw and in the thalamus in naïve wild-type animals and animals pretreated with lidocaine or saline. The numbers in the figure indicate the lidocaine dose in nmoles injected per mouse. All values are indicated as mean ± SEM ($^{*}P < 0.05$, $^{\#}P < 0.05$ compared to all other groups). (b) Relative withdrawal thresholds of the forepaws measured with dynamic von Frey filaments for mice injected with 3 nmole lidocaine (filled squares) or saline (open squares) at time t = 0. Values are given relative to average baseline value for the period −15 to 0 minutes (0.99 ± 0.04 g for lidocaine and 1.12 ± 0.08 g for saline group; not significantly different). An increased sensitivity was observed up to 40 minutes after lidocaine injection and up to 25 minutes after saline injection, the gray bar indicating the baseline range. All values are indicated as mean ± SEM, with * indicating a statistically significant difference at $P < 0.05$ level compared to baseline values, and # indicating a significant difference at $P < 0.05$ level between saline- and lidocaine-injected animals.

the stimulation periods; the heart rate (approximately 500 beats per minute) changed minimally at the onset of each stimulation period by 10–15 beats per minute, and returned to prestimulation values within <10 seconds.

Local administration of low doses of lidocaine into the mouse forepaw 40 minutes prior to the fMRI study led to a significant increase of the maximum BOLD signal change, as compared with the untreated forepaw stimulated at the same current amplitude. This is illustrated in Fig. 1, which includes activation maps and profiles for naïve mice and mice pretreated with 3 nmole of lidocaine. Yet, it should be noted that the intensity in activation maps indicates the value of the correlation with the model stimulation function and not the amplitude of the BOLD effect as such. Quantitative analysis of the fMRI signal revealed that the maximal BOLD signal change (in% of baseline values) in the S1 region contralateral to the stimulated paw in naïve animals was 2.9 ± 0.2% (n = 21, Figs. 1b, 2a). This differed significantly from the maximal BOLD values of 4.5 ± 0.2% (n = 28, $P < 0.0001$), 4.0 ± 0.6% (n = 7, $P = 0.05$), and 4.0 ± 0.7% (n = 7, $P = 0.04$) for 3, 4.5, and 6 nmole lidocaine dissolved in 10 μL, respectively, except for the lowest dose used (1.5 nmole), for which a value of 3.7 ± 0.4% (n = 8, $P = 0.1$) has been obtained. The BOLD response was dose dependent, with a maximum effect at 3 nmole of lidocaine injected locally (Fig. 2a). Clinically relevant doses (700 nmole, 2%) of lidocaine almost completely abolished the BOLD signal (0.7 ± 0.2%, n = 6; Figs. 1b, 2a). Activation maps for the 700-nmole lidocaine group derived from GLM analysis showed weak activation in the S1 area with clearly decreased intensity and extent, as compared with the untreated and low-dose lidocaine-treated groups (Fig. 1a). Injection of the vehicle (0.9% NaCl) led to a maximal BOLD signal change of 3.2 ± 0.3% (n = 6), which was not significantly different from the untreated animals ($P = 0.55$), but significantly smaller than the response following administration of 3 nmole lidocaine ($P = 0.03$; Fig. 2a). The maximum BOLD responses after injections of PBS or PBS with lidocaine were similar to the one observed after saline injection (3.6 ± 0.7%, 3.2 ± 0.6%, respectively), indicating no hyperalgesic effects (data not shown). The dependence on the lidocaine dose and the lack of response to the vehicle administration indicate that the increased sensitivity is caused by the local anesthetic administered at low concentrations.

To further validate these unexpected fMRI findings, we assessed the sensitivity of the mice in response to mechanical stimulation of the injected paw with von Frey filaments. In the saline group, the mean baseline forepaw withdrawal threshold of 1.2 ± 0.07 g was reduced to 0.5 ± 0.08 g ($P = 0.0008$) 10 minutes after saline injection and remained significantly lower for 25 minutes (0.5 ± 0.09 g, $P = 0.0008$) before slowly returning to baseline levels (Fig. 2b). The mean baseline values of the lidocaine group (1.0 ± 0.04 g) were

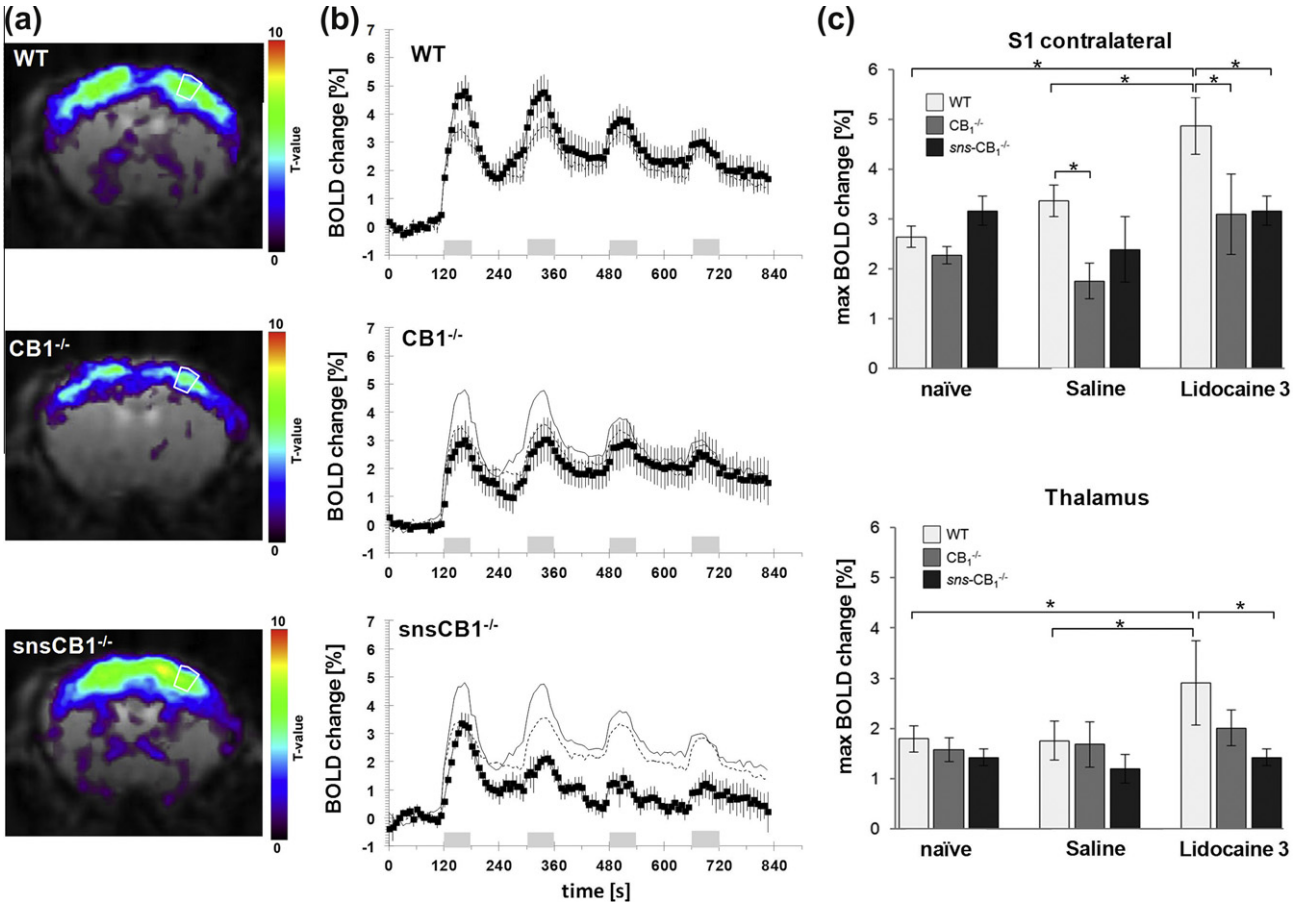

Fig. 3. Global and nociceptor-specific type 1 cannabinoid $(CB_1)^{-/-}$ mice do not show hyperalgesia after pretreatment with lidocaine. (a) Activity maps for brain slice (average group maps, 4.4 mm rostral to the interaural line) comprising somatosensory cortex S1 for wild-type (WT; top), $CB_1^{-/-}$ (middle), and *sns*-$CB_1^{-/-}$ mice (bottom) in response to electrical forepaw stimulation at 1.5 mA following local administration of lidocaine into the forepaw. (b) Blood oxygen level-dependent (BOLD) signal changes in% of baseline values in contralateral S1 cortical area indicated in (a) as a function of time for WT (top panel), $CB_1^{-/-}$ (middle panel) and *sns*-$CB_1^{-/-}$ mice (bottom panel) with electrical stimulation periods of the forepaw indicated as gray rectangles. For WT mice (top panel), curves represent the response to stimulation of the lidocaine- (filled symbols) and the saline-pretreated paw (dashed line, no symbols). In the lower 2 panels, the BOLD responses found in WT mice following lidocaine (solid line) and saline pretreatment (dashed line) are shown for comparison, illustrating the absence of an enhanced BOLD signal elicited by local administration of lidocaine in the 2 knockout mouse lines. (c) Maximum BOLD signal changes in the S1 contralateral to the stimulated paw and in the thalamus comparing WT (light gray bars), $CB_1^{-/-}$ (dark gray bars) and *sns*-$CB_1^{-/-}$ mice (black bars) with or without lidocaine pretreatment (3 nmole per mouse; "lidocaine 3"). The BOLD signal amplitudes in (b) and (c) show the absence of a hyperalgesic response to local lidocaine administration in $CB_1^{-/-}$ and *sns*-$CB_1^{-/-}$ mice, while this is not obvious from the activity maps. It should be noted, though, that activity maps indicate the strength of the correlation between the signal intensity and the model function for the stimulation rather than the amplitude of the effect. The reason for the better correlation in *sns*-$CB_1^{-/-}$ mice might be due to the faster return of the BOLD signal to baseline values. All values are indicated as mean ± SEM (*$P < 0.05$).

reduced to 0.3 ± 0.05 g ($P < 0.0001$) 5 minutes after injection of 3 nmole lidocaine solution. The reduced withdrawal threshold was observed for 40 minutes (0.6 ± 0.06 g, $P < 0.0001$) before increasing again slowly (Fig. 2b). The hyperalgesic effect was stronger and longer lasting in the lidocaine group as compared to the saline group, though only 2 time points were significantly different (Fig. 2b).

3.2. Lidocaine-induced hyperalgesia requires the CB_1 receptor

The hyperalgesic response induced by lidocaine pretreatment was investigated in global $CB_1^{-/-}$ mice and nociceptor-specific *sns*-$CB_1^{-/-}$ mice (Fig. 3). Analysis of the temporal profile in the contralateral S1 region revealed that the BOLD response in lidocaine-pretreated global $CB_1^{-/-}$ mice did not differ from the response observed in naïve WT animals, but was substantially reduced when compared to lidocaine-pretreated WT mice (Fig. 3b, middle panel). This is further corroborated by quantitative analysis: in global $CB_1^{-/-}$ mice, electrical stimulation of the forepaw at 1.5 mA yielded a maximal BOLD signal change of 2.3 ± 0.2% in S1 contralateral to the stimulated paw, indicating no significant difference of sensitivity as compared to WT animals ($P = 0.39$). Following pretreatment of the forepaws with 3 nmole lidocaine (10 μL), $CB_1^{-/-}$ mice did not show the hyperalgesic response observed in WT animals: the maximal BOLD values were 3.1 ± 0.8% in $CB_1^{-/-}$ vs 4.5 ± 0.2% in WT mice, which was statistically significantly different ($P = 0.01$). In contrast, there was no significant difference in BOLD signal amplitudes in $CB_1^{-/-}$ mice with and without lidocaine treatment ($P = 0.18$). Also, injection of 10 μL saline into the forepaw of the $CB_1^{-/-}$ mice did not affect the maximal BOLD signal change (1.8 ± 0.4%, $P = 0.08$) (Fig. 3c).

The involvement of the CB_1 receptor in eliciting the hyperalgesic response to lidocaine was confirmed by pharmacological inhibition of $CB_1^{-/-}$ receptors using the selective antagonist/inverse agonist rimonabant (Fig. 4). In the absence of lidocaine pretreatment, rimonabant did not affect the BOLD signal change (maximal amplitude in S1: 3.1 ± 0.4% with rimonabant vs 2.9 ± 0.2% without rimonabant, $P = 0.99$) in response to electrical stimulation. Systemic administration of rimonabant following pretreatment with 3 nmole lidocaine completely abolished the hyperalgesic effects of lidocaine (Fig. 4b, c) with maximal BOLD amplitudes in S1 of 3.2 ± 0.5% with rimonabant compared to 4.5 ± 0.2% without rimonabant ($P = 0.02$). In contrast, administration of the rimona-

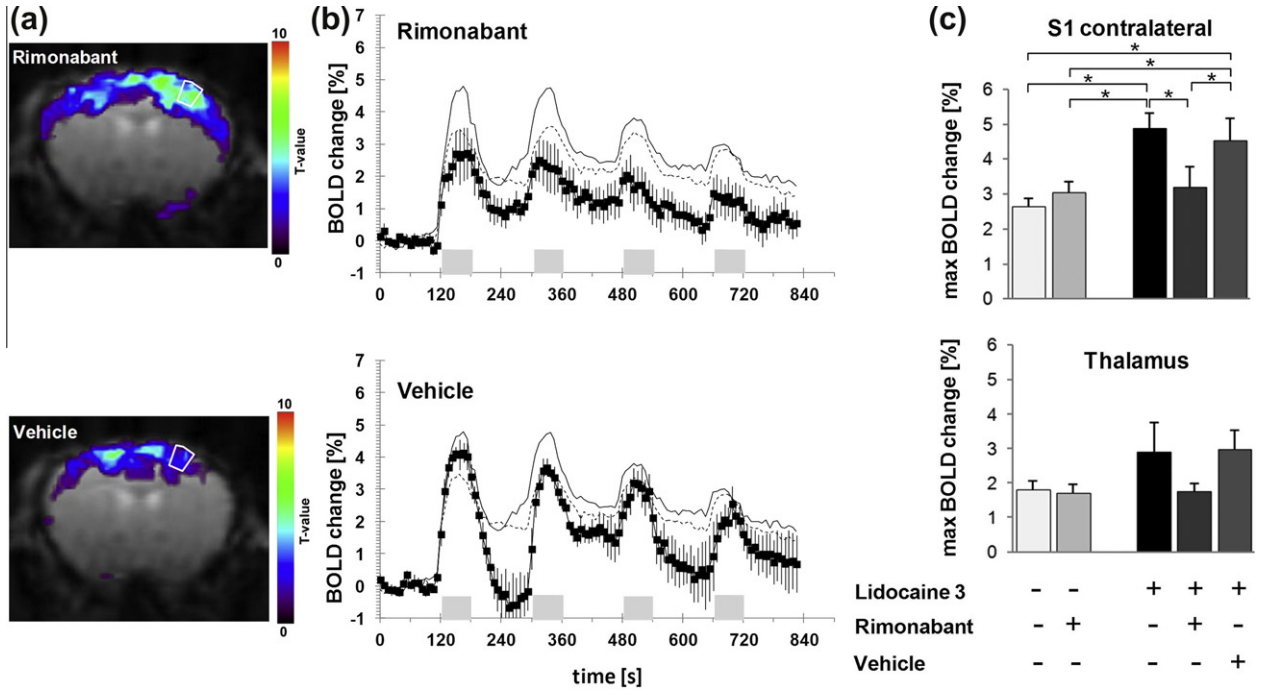

Fig. 4. Type 1 cannabinoid (CB_1) blocker rimonabant prevents development of hyperalgesia after pretreatment with lidocaine. (a) Activity maps for brain slice (average group maps, 4.4 mm rostral to the interaural line) comprising somatosensory cortex S1 in response to electrical forepaw stimulation at 1.5 mA for wild-type (WT) mice sensitized by local administration of lidocaine and treated by either intravenous administration of the CB_1 inhibitor rimonabant (upper) or vehicle (lower). (b) Relative blood oxygen level-dependent (BOLD) intensity in contralateral S1 cortical area indicated in (a) as a function of time for WT mice pretreated with lidocaine at a dose of 3 nmole (top panel) following intravenous administration of rimonabant (upper panel) or vehicle (lower panel). Periods for electrical stimulation are indicated as gray rectangles. For comparison, the BOLD response to electrical stimulation in WT mice pretreated with lidocaine (solid line) or saline (dashed line) only is included in the figures demonstrating that rimonabant inhibits the enhanced BOLD response due to lidocaine. (c) Maximum BOLD signal changes in the S1 contralateral to the stimulated paw and in the thalamus of naïve WT animals, WT mice treated with rimonabant only, an WT mice pretreated with lidocaine (3 nmole; "lidocaine 3"), lidocaine in combination with rimonabant and lidocaine in combination with vehicle. The BOLD signal amplitudes in (b) and (c) show the absence of a hyperalgesic response to local lidocaine administration in mice pretreated with rimonabant, while this is not obvious from the activity maps. All values are indicated as mean ± SEM (*$P < 0.05$).

bant vehicle did not reduce the hyperalgesic response to low-dose lidocaine and led to a maximal BOLD signal change in S1 of 4.5 ± 0.3%, which is comparable to the values observed following application of lidocaine alone (4.5 ± 0.2%, $P = 0.92$), but is significantly different from the application of rimonabant combined with lidocaine ($P = 0.02$) (Fig. 4c, upper panel).

Experiments with the nociceptor-specific *sns*-$CB_1^{-/-}$ mice indicated an important role of the CB_1 receptor in the periphery for the lidocaine-induced hyperalgesia. The response to electrical stimulation only (maximum amplitude contralateral S1: 3.18 ± 0.3%) was not significantly different from either the WT animals ($P = 0.5$) or the global $CB_1^{-/-}$ mice ($P = 0.07$). Electrical stimulation after lidocaine pretreatment led to a maximum BOLD signal amplitude in the S1 contralateral to the stimulated paw of 3.2 ± 0.3%, which was virtually identical to the values obtained with the global $CB_1^{-/-}$ mice after lidocaine treatment ($P = 0.9$; Fig. 3b, c), but significantly reduced compared to that observed in lidocaine-pretreated WT animals ($P = 0.001$).

For all experiments, the BOLD signal changes in the thalamus, a central region of the pain matrix, showed trends that are in line with the changes observed in the S1 region contralateral to the stimulated paw. This is reflected by the good correlation ($R^2 = 0.78$) of the BOLD responses (maximum amplitude) of the 2 regions.

4. Discussion

Functional MRI studies in humans and animals revealed noxious-evoked activation patterns that corresponded with the structures of the pain matrix [5,8,11,18,27,29,31,32], rendering fMRI an attractive modality for studying aspects of pain processing noninvasively. Due to the hemodynamic origin of the signal, activated areas derived from fMRI data analysis are usually not tightly confined to functional brain entities, but may include territories covered by irrigating and draining vessels. Correspondingly, activated areas in the mouse brain identified by fMRI correlation analysis (Fig. 1a) extend beyond functional territories derived from electrophysiological recordings displayed in brain atlases [15].

Lidocaine is a widely used local anesthetic and antiarrhythmic agent, which acts primarily through inhibition of voltage-gated sodium channels. These channels play a crucial role in generation and propagation of action potentials. Blocking sodium channels by lidocaine inhibits signal propagation along nerve fibers and therefore should abolish a functional response in the CNS. In fact, in our study, local administration of lidocaine at clinical doses (2%, ie, 700 nmole per mouse) prior to the stimulation experiment largely abolished the cerebral BOLD response.

Administration of lidocaine at low doses, however, caused significant and reproducible hyperalgesia, a surprising observation for a compound clinically used for analgesia. Similar observations have been reported previously [28,40]. We found doses of lidocaine between 3 and 6 nmole to elicit significant increases in local brain activity as reflected by increased amplitude and spatial extent of the BOLD signal. This sensitization following low-dose lidocaine injection could be reproduced in all animals studied with the von Frey filament test. The hyperalgesic effect did not last quite as long as in the fMRI experiments, most likely because mice were awake and moving in the behavioral test, while animals in the fMRI experiments were anesthetized.

The underlying mechanisms acting in the sensory afferents are not entirely understood. Experiments with injection of saline indicate a slight, though not significant, increase of the BOLD response. This largely excludes the increased amount of liquid and

electrolytes in the paw, which might alter electrical conductivity, to be the cause for the hyperalgesic response observed. This was also supported by behavioral testing: saline injection led to decreased withdrawal thresholds, but the sensitization was less pronounced and shorter lasting than that observed after lidocaine injection. Saline-induced sensitization may be caused by effects due to NaCl itself, changes in pH, or by mechanical irritation from the injection, all factors that also apply to lidocaine injections. fMRI measurements using PBS (pH 7.4) alone or with 3 nmole lidocaine (pH 7.3) led to a maximum BOLD amplitude after electrical stimulation similar to that observed after injection of unbuffered saline and not significantly different from that without any pretreatment (data not shown). Accordingly, the sensitizing effect cannot be attributed solely to local tissue acidification. As the buffering capacity of lidocaine at the doses used in our studies is very low, it is unlikely that differences in extent and time course of the hyperalgesic response between lidocaine and saline treatment can be attributed to differences in tissue pH dynamics. It appears that only the combination of reduced pH (around 6.3) and lidocaine induces hyperalgesia, as neither saline alone (low pH) nor lidocaine in PBS (pH 7.4) led to a significant sensitization.

The observations that, in global $CB_1^{-/-}$ mice, the BOLD response to electrical stimulation was not affected by administration of 3 nmole lidocaine (the dose eliciting the largest effect in WT animals) and that the lidocaine-induced hyperalgesic effect could be completely inhibited by administration of the CB_1 receptor blocker rimonabant, clearly demonstrate an involvement of the endocannabinoid system in the development of this type of hyperalgesia. Experiments performed with nociceptor-specific *sns*-$CB_1^{-/-}$ mice indicate a crucial role of the CB_1 receptors located on the nociceptors. The fact that *sns*-$CB_1^{-/-}$ mice behaved similarly to the global $CB_1^{-/-}$ mice and also did not display lidocaine-induced hyperalgesia suggests a peripheral sensitization mechanism. CB_1 receptor involvement was deduced from the analysis of BOLD signal amplitudes in activated areas rather than from activity maps. Activity maps indicate the strength of the correlation between the signal intensity in a voxel and the model function describing the stimulation paradigm and do not necessarily reflect the amplitude of the response.

It has previously been shown that in cells expressing both CB1 and TRPV1 receptors, CB1 activation either inhibits or stimulates TRPV1, depending on activation of the cAMP cascade [19]. A recent report by Fioravanti et al. [14] showed that a direct interaction with the CB_1 receptor maintains TRPV1 channel in a sensitized state. We hypothesized that the initial local injection of lidocaine at low doses led to sensitization of the TRPV1 receptors, either through direct activation or induced by the low pH (6.3) of the solutions. The peripheral CB_1 receptors seem to play a role in eliciting or maintaining the TRPV1 sensitization, which prompts an increased BOLD response to electrical stimulation.

At pH 6.3, protons do not directly activate the TRPV1 channel, but rather act as modulators rendering it more sensitive, for example, to heat. Patch-clamp experiments on TRPV1-transfected cells showed that at pH 6.4, body temperature (37°C) is already sufficient to induce activation of the sensitized channel [21,39]. However, the temperature measured at the forepaw during the time point of injection was around 30°C, which is markedly lower and therefore unlikely to induce TRPV1 activation. We therefore conclude that sensitized TRPV1 receptors get activated directly by lidocaine, a mechanism which has been shown earlier for higher concentrations of lidocaine [25]. These findings are supported by the fact that injections of the saline solutions of the same pH value only led to a short-lasting sensitization in the von Frey behavioral test. Also, fMRI measurements using electrical stimulation did not reveal hyperalgesic effects at 40 minutes following saline injection only, in contrast to the increased response observed 40 minutes after the injection of lidocaine dissolved in saline.

Other mechanisms might also contribute to the hyperalgesic effect observed in fMRI experiments following administration of lidocaine at low doses. Lidocaine inhibits tandem pore domain potassium channels at concentrations similar to those required for sodium channel block with EC50s of about 200 μM ([6,7,23,36]). Block of tandem pore domain potassium channels might lead to a change in excitability of primary nociceptors and enhance their sensitivity to noxious input. Whether these channels interact also with CB_1 receptors is at present not known.

Independent of these potential peripheral mechanisms leading to a sensitization, central mechanisms have been suggested. Pernía-Andrade et al. demonstrated the activation of CB_1 receptors of the dorsal horn in the spinal cord during strong nociceptive (C-fiber) input [37]. This would cause a disinhibition of pain-specific neurons in the dorsal horn, which are rendered sensitive to input even from nonnociceptive A-fibers, thereby resulting in hyperalgesia in areas surrounding the original nociceptive input. While we cannot exclude contribution from this central CB_1 mechanism, our experimental findings are consistent with the activation of CB_1 receptors located at peripheral nociceptors.

fMRI studies are typically carried out in anesthetized animals, a recurring issue, in particular when investigating nociception. Ideally, anesthesia should neither interfere with brain activity nor act as analgesic. However, many anesthetics suitable for longitudinal studies have an analgesic component, and some even affect the neurovascular coupling. We used isoflurane as it allows easy administration and controlled dosing. In previous studies, we [5] and others [13,20,33] have shown that robust and reproducible fMRI signals can be obtained in response to sensory and noxious stimuli; in the latter case, significant activation has been observed in brain areas involved in pain processing, indicating feasibility of such studies using this anesthesia protocol. Yet, it has been suggested that the endocannabinoid system might interact with isoflurane-induced anesthesia, though this claim is not yet sufficiently substantiated with data. While activation of CB_1 is known to decrease GABAergic inhibition of synaptic transmission in most brain regions [22], volatile anesthetics may enhance GABA-A receptor-mediated inhibition [17]; hence, a putative interaction cannot be excluded.

4.1. Conclusion

In summary, modulation of nociceptive processing by local anesthetic lidocaine was investigated in mice using fMRI. The response to a nociceptive peripheral stimulus was quantitatively analyzed with regard to both amplitude and spatial extent of the BOLD signal change. It could be demonstrated that lidocaine at low dose induced reproducible hyperalgesia. Studies in transgenic mice lacking the CB_1 receptor ubiquitously (global $CB_1^{-/-}$) or on peripheral nociceptors (*sns*-$CB_1^{-/-}$) indicated that this effect was predominantly mediated by CB_1 receptors expressed on nociceptors.

Aside from the mechanistic implications, these findings might also be of clinical relevance. Therapeutically used solutions of lidocaine have pH values of 6.2–6.6 [12], which is in the range of the solutions applied in this study. In spite of the higher concentrations of lidocaine applied clinically, there will be regions in the boundary area of the infiltrated tissue, in which concentrations are as low as the ones used in this study. Similarly, in the course of drug washout and degradation, low concentrations of lidocaine will inevitably occur. The observation that such low concentrations can cause a sensitization may relate to postsurgical hyperalgesia [40].

Conflicts of interest statement

There are no conflicts of interest to declare.

Acknowledgements

The authors thank B. Lutz and G. Marsicano for providing the $CB_1^{-/-}$ mice, and R. Kuner for providing the *sns*-$CB_1^{-/-}$ mice. The project was funded by the National Center of Competence in Research (NCCR) "Neural Plasticity and Repair," Switzerland and the Swiss National Science Foundation (Grant 126029).

References

[1] Adamczak JM, Farr TD, Seehafer JU, Kalthoff D, Hoehn M. High field BOLD response to forepaw stimulation in the mouse. Neuroimage 2010;51:704–12.
[2] Agarwal N, Pacher P, Tegeder I, Amaya F, Constantin CE, Brenner GJ, Rubino T, Michalski CW, Marsicano G, Monory K, Mackie K, Marian C, Batkai S, Parolaro D, Fischer MJ, Reeh P, Kunos G, Kress M, Lutz B, Woolf CJ, Kuner R. Cannabinoids mediate analgesia largely via peripheral type 1 cannabinoid receptors in nociceptors. Nat Neurosci 2007;10:870–9.
[3] Apkarian AV, Bushnell MC, Treede RD, Zubieta JK. Human brain mechanisms of pain perception and regulation in health and disease. Eur J Pain 2005;9:463–84.
[4] Baltes C, Radzwill N, Bosshard SC, Marek D, Rudin M. Micro MRI of the mouse brain using a novel 400 MHz cryogenic quadrature RF probe. NMR Biomed 2009;22:834–42.
[5] Bosshard SC, Baltes C, Wyss MT, Mueggler T, Weber B, Rudin M. Assessment of brain responses to innocuous and noxious electrical forepaw stimulation in mice using BOLD fMRI. Pain 2010;151:655–63.
[6] Bräu ME, Nau C, Hempelmann G, Vogel W. Local anesthetics potently block a potential insensitive potassium channel in myelinated nerve. J Gen Physiol 1995;105:485–505.
[7] Bräu ME, Vogel W, Hempelmann G. Fundamental properties of local anesthetics: half-maximal blocking concentrations for tonic block of Na^+ and K^+ channels in peripheral nerve. Anesth Analg 1998;87:885–9.
[8] Casey KL. Forebrain mechanisms of nociception and pain: analysis through imaging. Proc Natl Acad Sci USA 1999;96:7668–74.
[9] Caterina MJ, Leffler A, Malmberg AB, Martin WJ, Trafton J, Petersen-Zeitz KR, Koltzenburg M, Basbaum AI, Julius D. Impaired nociception and pain sensation in mice lacking the capsaicin receptor. Science 2000;288:306–13.
[10] Caterina MJ, Schumacher MA, Tominaga M, Rosen TA, Levine JD, Julius D. The capsaicin receptor: a heat-activated ion channel in the pain pathway. Nature 1997;389:816–24.
[11] Davis KD, Taylor SJ, Crawley AP, Wood ML, Mikulis DJ. Functional MRI of pain- and attention-related activations in the human cingulate cortex. J Neurophysiol 1997;77:3370–80.
[12] Documed. Arzneimittel-Kompendium der Schweiz. Basel, Switzerland: Documed AG; 2011.
[13] Endo T, Spenger C, Westman E, Tominaga T, Olson L. Reorganization of sensory processing below the level of spinal cord injury as revealed by fMRI. Exp Neurol 2008;209:155–60.
[14] Fioravanti B, De Felice M, Stucky CL, Medler KA, Luo MC, Gardell LR, Ibrahim M, Malan Jr TP, Yamamura HI, Ossipov MH, King T, Lai J, Porreca F, Vanderah TW. Constitutive activity at the cannabinoid CB1 receptor is required for behavioral response to noxious chemical stimulation of TRPV1: antinociceptive actions of CB1 inverse agonists. J Neurosci 2008;28:11593–602.
[15] Franklin K, Paxinos G. The mouse brain in stereotaxic coordinates. 2nd ed. San Diego: Academic Press; 2001.
[16] Harvey RJ, Depner UB, Wassle H, Ahmadi S, Heindl C, Reinold H, Smart TG, Harvey K, Schutz B, Abo-Salem OM, Zimmer A, Poisbeau P, Welzl H, Wolfer DP, Betz H, Zeilhofer HU, Müller U. GlyR alpha 3: an essential target for spinal PGE2-mediated inflammatory pain sensitization. Science 2004;304:884–7.
[17] Haseneder R, Rammes G, Zieglgänsberger W, Kochs E, Hapfelmeier G. GABA(A) receptor activation and open-channel block by volatile anaesthetics: a new principle of receptor modulation? Eur J Pharmacol 2002;451:43–50.
[18] Heindl-Erdmann C, Axmann R, Kreitz S, Zwerina J, Penninger J, Schett G, Brune K, Hess A. Combining functional magnetic resonance imaging with mouse genomics: new options in pain research. Neuroreport 2010;21:29–33.
[19] Hermann H, De Petrocellis L, Bisogno T, Schiano Moriello A, Lutz B, Di Marzo V. Dual effect of cannabinoid CB1 receptor stimulation on a vanilloid VR1 receptor-mediated response. Cell Mol Life Sci 2003;60:607–16.
[20] Hess A, Sergejeva M, Budinsky L, Zeilhofer HU, Brune K. Imaging of hyperalgesia in rats by functional MRI. Eur J Pain 2007;11:109–19.
[21] Jordt SE, Tominaga M, Julius D. Acid potentiation of the capsaicin receptor determined by a key extracellular site. Proc Natl Acad Sci USA 2000;97:8134–9.
[22] Katona I, Rancz EA, Acsady L, Ledent C, Mackie K, Hajos N, Freund TF. Distribution of CB1 cannabinoid receptors in the amygdala and their role in the control of GABAergic transmission. J Neurosci 2001;21:9506–18.
[23] Kindler CH, Yost CS, Gray AT. Local anesthetic inhibition of baseline potassium channels with two pore domains in tandem. Anesthesiology 1999;90:1092–102.
[24] Ledent C, Valverde O, Cossu G, Petitet F, Aubert JF, Beslot F, Boehme GA, Imperato A, Pedrazzini T, Roques BP, Vassart G, Fratta W, Parmentier M. Unresponsiveness to cannabinoids and reduced addictive effects of opiates in CB1 receptor knockout mice. Science 1999;283:401–4.
[25] Leffler A, Fischer MJ, Rehner D, Kienel S, Kistner K, Sauer SK, Gavva NR, Reeh PW, Nau C. The vanilloid receptor TRPV1 is activated and sensitized by local anesthetics in rodent sensory neurons. J Clin Invest 2008;118:763–76.
[26] Leite CE, Mocelin CA, Petersen GO, Leal MB, Thiesen FV. Rimonabant: an antagonist drug of the endocannabinoid system for the treatment of obesity. Pharmacol Rep 2009;61:217–24.
[27] Lilja J, Endo T, Hofstetter C, Westman E, Young J, Olson L, Spenger C. Blood oxygenation level-dependent visualization of synaptic relay stations of sensory pathways along the neuroaxis in response to graded sensory stimulation of a limb. J Neurosci 2006;26:6330–6.
[28] Luo Z, Yu M, Smith SD, Kritzer M, Du C, Ma Y, Volkow ND, Glass PS, Benveniste H. The effect of intravenous lidocaine on brain activation during non-noxious and acute noxious stimulation of the forepaw: a functional magnetic resonance imaging study in the rat. Anesth Analg 2009;108:334–44.
[29] Manning BH, Morgan MJ, Franklin KB. Morphine analgesia in the formalin test: evidence for forebrain and midbrain sites of action. Neuroscience 1994;63:289–94.
[30] Marsicano G, Wotjak CT, Azad SC, Bisogno T, Rammes G, Cascio MG, Hermann H, Tang J, Hofmann C, Zieglgänsberger W, Di Marzo V, Lutz B. The endogenous cannabinoid system controls extinction of aversive memories. Nature 2002;418:530–4.
[31] Millan MJ. The induction of pain: an integrative review. Prog Neurobiol 1999;67:1–164.
[32] Morrow TJ, Paulson PE, Danneman PJ, Casey KL. Regional changes in forebrain activation during the early and late phase of formalin nociception: analysis using cerebral blood flow in the rat. Pain 1998;75:355–65.
[33] Nair G, Duong TQ. FMRI of mice on a narrow-bore 9.4 T magnet. Magn Reson Med 2004;52:430–4.
[34] Nassar MA, Stirling LC, Forlani G, Baker MD, Matthews EA, Dickenson AH, Wood JN. Nociceptor-specific gene deletion reveals a major role for Nav1.7 (PN1) in acute and inflammatory pain. Proc Natl Acad Sci USA 2004;101:12706–11.
[35] Ogawa S, Lee TM, Nayak AS, Glynn P. Oxygenation-sensitive contrast in magnetic resonance image of rodent brain at high magnetic fields. Magn Reson Med 1990;14:68–78.
[36] Olschewski A, Wolff M, Brau ME, Hempelmann G, Vogel W, Safronov BV. Enhancement of delayed-rectifier potassium conductance by low concentrations of local anaesthetics in spinal sensory neurones. Br J Pharmacol 2002;136:540–9.
[37] Pernía-Andrade AJ, Kato A, Witschi R, Nyilas R, Katona I, Freund TF, Watanabe M, Filitz J, Koppert W, Schüttler J, Ji G, Neugebauer V, Marsicano G, Lutz B, Vanegas H, Zeilhofer HU. Spinal endocannabinoids and CB1 receptors mediate C-fiber-induced heterosynaptic pain sensitization. Science 2009;325:760–4.
[38] Sydekum E, Baltes C, Ghosh A, Mueggler T, Schwab ME, Rudin M. Functional reorganization in rat somatosensory cortex assessed by fMRI: elastic image registration based on structural landmarks in fMRI images and application to spinal cord injured rats. Neuroimage 2009;44:1345–54.
[39] Tominaga M, Caterina MJ, Malmberg AB, Rosen TA, Gilbert H, Skinner K, Raumann BE, Basbaum AI, Julius D. The cloned capsaicin receptor integrates multiple pain-producing stimuli. Neuron 1998;21:531–43.
[40] Wilder-Smith OHG, Arendt-Nielsen L. Postoperative hyperalgesia: its clinical importance and relevance. Anesthesiology 2006;104:601–7.
[41] Woolf CJ. Pain: moving from symptom control toward mechanism-specific pharmacologic management. Ann Intern Med 2004;140:441–51.
[42] Zhao F, Williams M, Welsh DC, Meng X, Ritter A, Abbadie C, Cook JJ, Reicin AS, Hargreaves R, Williams DS. FMRI investigation of the effect of local and systemic lidocaine on noxious electrical stimulation-induced activation in the spinal cord. Pain 2009;145:110–9.